

The Fe-Cu System: A Thermodynamic Evaluation

QING CHEN and ZHANPENG JIN

Thermochemical and phase diagram data in the Fe-Cu system have been critically evaluated by using phenomenological models for the Gibbs energy of various phases. A set of thermodynamic parameters more consistent with most of the selected experimental data than previous assessments has been obtained by a computerized least-squares method. Stable and metastable phase equilibria, T_0 curves, and thermodynamic properties are calculated with the optimized parameters. The calculated liquid/face-centered cubic (fcc) T_0 curve and metastable liquid spinodal seem to permit an accurate prediction of maximum solid solubility obtained upon melt quenching in this system.

I. INTRODUCTION

THE Fe-Cu system, which is of considerable technological importance, has been extensively assessed.^[1-5] However, as remarked by Chuang, Schmid, and Chang,^[5] the agreement between these assessments and the experimental phase diagram data is still not satisfactory enough in the high temperature range of the system. Moreover, combination of these assessments with many other binary systems assessed recently for extrapolation to higher order systems is impossible because the unary data and thermodynamic models they employed are different from what were generally accepted for the present. It is the main aim of the present study to provide a revised critical assessment of the thermochemical and phase diagram data in the Fe-Cu system with use of the thermodynamical models widely adopted and unary data recently compiled by Dinsdale^[6] and to present a set of parameters satisfactory for reproducing most of the experimental data on thermodynamic properties and phase diagrams simultaneously. Some metastable phase equilibria and T_0 curves also will be calculated by taking advantage of the optimized parameters. The calculated liquid/fcc T_0 curve and metastable liquid spinodal will be utilized readily to shed light on the limit of enhanced solid solubility upon rapid solidification from melt in this system.

The assessment technique applied in this work is the so-called calculation of phase diagrams (CALPHAD) method.^[7] It includes choice of models for the Gibbs energy of various phases, selection of experimental data, and computerized evaluation of the model parameters.

II. THERMODYNAMIC MODELS

The Fe-Cu binary system consists of three condensed phases, namely, liquid, face-centered cubic (fcc), and body-centered cubic (bcc). In common practice, the Fe-rich fcc phase is designated as γ , the Cu-rich fcc as ϵ , the high temperature bcc as δ , and the low temperature bcc as α .

QING CHEN, Ph.D. Candidate, and ZHANPENG JIN, Professor, are with the Department of Materials Science and Engineering, the Central South University of Technology, Changsha, Hunan 410083, People's Republic of China.

Manuscript submitted July 29, 1993.

A. Liquid Phase

The liquid phase was described with a substitutional solution model, which yields the Gibbs energy per mole of atoms in the following form:

$$G_m^{\text{liq}} = x_{\text{Fe}} \circ G_{\text{Fe}}^{\text{liq}} + x_{\text{Cu}} \circ G_{\text{Cu}}^{\text{liq}} + RT (x_{\text{Fe}} \ln x_{\text{Fe}} + x_{\text{Cu}} \ln x_{\text{Cu}}) + {}^E G_m^{\text{liq}} \quad [1]$$

where x_i is the atomic fraction of component i , $\circ G_i^{\text{liq}}$ is the Gibbs energy of pure element i in liquid state, and ${}^E G_m^{\text{liq}}$ is the excess Gibbs energy. The $\circ G_i^{\text{liq}}$ values were taken from Dinsdale^[6] for the present study, and ${}^E G_m^{\text{liq}}$ was given by a Redlich-Kister polynomial, expressed as follows:

$${}^E G_m^{\text{liq}} = x_{\text{Fe}} x_{\text{Cu}} \sum_{i=0}^n L_{\text{Fe,Cu}}^{\text{liq},i} (x_{\text{Fe}} - x_{\text{Cu}})^i \quad [2]$$

Each interaction parameter $L_{\text{Fe,Cu}}^{\text{liq},i}$ ($i = 0, 1, 2, \dots, n$) may be a constant or may vary, in general linearly, with temperature. The actual choice of $L_{\text{Fe,Cu}}^{\text{liq},i}$ was made by trial and error during the assessment work and represents a compromise between an accurate description of the selected information and the desire of working with a few statistically significant parameters.

B. fcc and bcc Phases

The Gibbs energy of the fcc and bcc phases was described by resolving it into a magnetic (ΔG_m^{mg}) and a nonmagnetic contribution. The magnetic contribution was represented using a model proposed by Inden^[8] and modified by Hillert and Jarl,^[9] whereas the nonmagnetic contribution was described in the same way as the molar Gibbs energy of the liquid phase. Thus, the Gibbs energy per mole of atoms for the phase Φ ($\Phi = \text{fcc}, \text{bcc}$) is written as

$$G_m^\Phi = x_{\text{Fe}} \circ G_{\text{Fe}}^\Phi + x_{\text{Cu}} \circ G_{\text{Cu}}^\Phi + RT (x_{\text{Fe}} \ln x_{\text{Fe}} + x_{\text{Cu}} \ln x_{\text{Cu}}) + {}^E G_m^{\text{mg},\Phi} + \Delta G_m^{\text{mg},\Phi} \quad [3]$$

Here, the quantity $\circ G_i^\Phi$ is the Gibbs energy of component i with the structure of phase Φ in a hypothetical nonmagnetic state, and its value was taken from Dinsdale.^[6] The excess Gibbs energy ${}^E G_m^{\text{mg},\Phi}$ was expressed by Eq. [2] by replacing the suffix liq with Φ , *i.e.*,

$$E_{G_m}^{\phi} = x_{Fe}x_{Cu} \sum_{i=0}^n i L_{Fe,Cu}^{\phi} (x_{Fe} - x_{Cu})^i \quad [4]$$

The last term in Eq. [3], $\Delta G_m^{mg,\phi}$, representing the magnetic contribution to the Gibbs energy, is given by the expression

$$\Delta G_m^{mg,\phi} = RT (\ln \beta^{\phi} + 1) f(\tau^{\phi}) \quad [5]$$

where β^{ϕ} is a quantity related to the total magnetic entropy as follows:

$$\Delta S_m^{mg}(\infty) - \Delta S_m^{mg}(0) = R \ln (\beta^{\phi} + 1) \quad [6]$$

The variable τ^{ϕ} is defined as T/T_c^{ϕ} , where T_c^{ϕ} is the critical temperature for magnetic ordering of the structure Φ at a given composition, *i.e.*, the Curie temperature for ferromagnetic ordering or the Neel temperature (T_N) for antiferromagnetic ordering. The function $f(\tau^{\phi})$ represents the polynomial proposed by Hillert and Jarl,^[9] which is given in Table I.

When applying Eq. [5] to alloys, the composition dependence of the quantities T_c^{ϕ} and β^{ϕ} has to be accounted for. This was done by adopting the following expressions:

$$T_c^{\phi} = x_{Fe}T_{cFe}^{\phi} + x_{Cu}T_{cCu}^{\phi} + x_{Fe}x_{Cu}T_{cFe,Cu}^{\phi} \quad [7]$$

$$\beta^{\phi} = x_{Fe}\beta_{Fe}^{\phi} + x_{Cu}\beta_{Cu}^{\phi} + x_{Fe}x_{Cu}\beta_{Fe,Cu}^{\phi} \quad [8]$$

Here, T_{ci}^{ϕ} and β_i^{ϕ} are the critical temperature and the quantity related to the total magnetic entropy for pure element i with structure Φ , respectively, and $T_{cFe,Cu}^{\phi}$ and $\beta_{Fe,Cu}^{\phi}$ are the phenomenological parameters to be evaluated from experimental data. In the present work, the values of T_{cFe}^{ϕ} and β_{Fe}^{ϕ} were taken from the study by Guillermet,^[10] those of T_{cCu}^{ϕ} and β_{Cu}^{ϕ} were set to zero; $T_{Fe,Cu}^{bcc}$ was evaluated from the experimental work by Ruer and Goerens,^[11] and the rest, $T_{cFe,Cu}^{fcc}$, $\beta_{Fe,Cu}^{bcc}$, and $\beta_{Fe,Cu}^{fcc}$, with no experimental information to fit, were set arbitrarily to zero. All of the magnetic parameters with nonzero values are summarized in Table I.

III. SELECTION OF EXPERIMENTAL DATA AND PARAMETERS EVALUATION

The interaction parameters in the thermodynamic models are evaluated by searching for the best fit to the selected experimental data on both phase diagram and thermochemical properties. All fits to the experimental quantities were performed by using a computer optimization program called BINGSS.^[12] This program can treat various types of input data simultaneously and optimize the parameters by minimizing the sum of squares of the differences between experimental and calculated values. Each piece of experimental information was given a certain weight in the optimization. The weights were chosen by personal judgement and changed by trial and error during the work until most of the input information was accounted for within the expected uncertainty limits. During this work, optimizations were made in steps in which only one subset of input data was included. After a preliminary description of the phase

under consideration was evaluated in each step, all selected input values were included in a same optimization to obtain the final results.

The experimental information has been reviewed by Hansen and Anderko,^[13] Elliott,^[14] Shunk,^[15] Hultgren *et al.*,^[16] Kubaschewski *et al.*,^[1] and Chuang *et al.*^[5] Here, we shall only summarize the data we adopted for parameters evaluation. The temperature values reported on the IPTS-48 scale in the literature are corrected to the IPTS-68 temperature scale by applying a standard conversion method^[17] when they are accepted in the optimization.

A. Phase Diagram Data

1. Solid/liquid equilibria

By means of thermal analysis and microstructure examination, Maddocks and Claussen^[18] have investigated the system above 800 K within the whole composition range and Hellawell and Hume-Rothery^[19] have investigated the system at high temperatures for the Fe-rich compositions. It seems that the latter group gave systematically lower temperatures for the liquidus and peritectic reactions than the former. In the present assessment, the liquidus data and peritectic temperatures measured by Maddocks and Claussen,^[18] which were accepted by Hansen and Anderko,^[13] are preferred. Experimental information on the metastable liquid miscibility gap and liquidus curve in the middle composition range was reported by Nakagawa^[20] from the measurement of magnetic susceptibility and the microscopic observation in 1958, which confirms the near-flatness of the liquidus at temperatures between 1700 and 1710 K. As for the solidus of the γ phase, a retrograde curve rather than the vertical line defined by Maddocks and Claussen^[18] and Hellawell and Hume-Rothery^[19] is obtained by Olsen *et al.*^[21] through quantitative thermal analysis, which was later supported by the Electron Probe Microanalysis (EPMA) data from Bochvar *et al.*,^[22] Hasebe and Nishizawa,^[2] and Lindqvist and Uhrenius.^[3] Olsen *et al.*,^[21] Hasebe and Nishizawa,^[2] and Lindqvist and Uhrenius^[3] have also contributed to the liquidus data for the γ phase.

2. Solid/solid equilibria

The γ solvus has been well determined with EMPA by Speich *et al.*,^[23] Salje and Feller-Kniepmeier,^[24] and Hasebe and Nishizawa.^[2] Speich *et al.*^[23] and Salje and Feller-Kniepmeier^[24] have also determined the Cu solubility in α phase, for which earlier work had been done by Wriedt and Darken^[25] using saturation method and chemical analysis and by Qureshi^[26] through the measurement of initial permeability and electric resistivity.

The experimental information on the solubility of Fe in ϵ phase has been obtained by Tammann and Olsen^[27] using a magnetic method, by Andersen and Kingsbury^[28] using X-ray, and by Salje and Feller-Kniepmeier^[24] and Hasebe and Nishizawa^[2] using EMPA.

For the temperature of the eutectoid equilibrium, $\gamma \rightleftharpoons \alpha + \epsilon$, the recommended value by Speich *et al.*^[23] was included as the starting one.

Table I. Summary of Thermodynamic Parameters in the Fe-Cu System. All Values Are in SI Units Per One Mole of Atoms of Each Phase. The Functions Are Valid for 298.15 < T < 6000 K Unless Otherwise Stated.

The magnetic contribution to Gibbs energy is described by $\Delta G_m^{mg} = RT \ln (\beta + 1)f(\tau)$, where $\tau = T/T_c$. The term T_c is the Curie or Neel temperature and β is related to the total magnetic entropy. Negative values of T_c and β are used to characterize the properties of an antiferromagnetic phase and should be divided by -1 for bcc and by -3 for fcc and hcp when inserting them in ΔG_m^{mg} and $f(\tau)$. The value of $f(\tau)$ is given as follows:

$$f(\tau) = 1 - \frac{1}{A} \left[\frac{79\tau^{-1}}{140P} + \frac{158}{497} \left(\frac{1}{P} - 1 \right) \left(\frac{\tau^3}{2} + \frac{\tau^9}{45} + \frac{\tau^{15}}{200} \right) \right] \quad \tau < 1$$

$$= -\frac{1}{A} \left[\frac{\tau^{-5}}{10} + \frac{\tau^{-15}}{315} + \frac{\tau^{-25}}{1500} \right] \quad \tau > 1$$

where $A = \frac{518}{1125} + \frac{11,692}{15,975} \left(\frac{1}{P} - 1 \right)$ and P depends on the structure. For bcc, $P = 0.40$, and for fcc and hcp $P = 0.28$.

$$H_{Fe}^{SER} = 4489.0 \quad H_{Cu}^{SER} = 5004.0$$

Liquid phase:

$${}^0G_{Fe}^{liq} - H_{Fe}^{SER} = 13,265 + 117.57557 T - 23.5143 T \ln T - 0.00439752 T^2 - 5.89269 \cdot 10^{-8} T^3 + 77,358.5 T^{-1} - 3.675155 \cdot 10^{-21} T^7 \quad \begin{matrix} 298.15 < T < 1811 \\ 1811 < T < 6000 \end{matrix}$$

$$= -10,839.7 + 291.302 T - 46.0 T \ln T$$

$${}^0G_{Cu}^{liq} - H_{Cu}^{SER} = 5194.34 + 120.97476 T - 24.1124 T \ln T - 0.00265684 T^2 + 1.29223 \cdot 10^{-7} T^3 + 52,477.8 T^{-1} - 5.83932 \cdot 10^{-21} T^7 \quad \begin{matrix} 298.15 < T < 1358 \\ 1358 < T < 6000 \end{matrix}$$

$$= -46.9 + 173.88354 T - 31.38 T \ln T$$

$${}^0L_{Fe,Cu}^{liq} = 35,625.8 - 2.19045 T$$

$${}^1L_{Fe,Cu}^{liq} = 1529.8 - 1.15291 T$$

$${}^2L_{Fe,Cu}^{liq} = 12,714.4 - 5.18624 T$$

$${}^3L_{Fe,Cu}^{liq} = -1177.1$$

Fcc phase:

$${}^0G_{Fe}^{fcc} - H_{Fe}^{SER} = -237.57 + 132.416 T - 24.6643 T \ln T - 0.00375752 T^2 - 5.89269 \cdot 10^{-8} T^3 + 77358.5 T^{-1} \quad \begin{matrix} 298.15 < T < 1811 \\ 1811 < T < 6000 \end{matrix}$$

$$= -27,098.266 + 300.25256 T - 46.0 T \ln T + 2.78854 \cdot 10^{31} T^{-9}$$

$${}^0G_{Cu}^{fcc} - H_{Cu}^{SER} = -7770.46 + 130.485 T - 24.1124 T \ln T - 0.00265684 T^2 + 1.29223 \cdot 10^{-7} T^3 + 52,477.8 T^{-1} \quad \begin{matrix} 298.15 < T < 1358 \\ 1358 < T < 6000 \end{matrix}$$

$$= -13,542.3 + 183.804 T - 31.38 T \ln T + 3.64643 \cdot 10^{29} T^{-9}$$

$${}^0L_{Fe,Cu}^{fcc} = 43,319.6 - 6.94445 T$$

$${}^1L_{Fe,Cu}^{fcc} = -6068.8 + 2.83662 T$$

$${}^2L_{Fe,Cu}^{fcc} = 3629.4$$

$$T_c^{fcc} = -201 x_{Fe}$$

$$\beta^{fcc} = -2.1 x_{Fe}$$

Bcc phase:

$${}^0G_{Fe}^{bcc} - H_{Fe}^{SER} = 1224.83 + 124.134 T - 23.5143 T \ln T - 0.00439752 T^2 - 5.89269 \cdot 10^{-8} T^3 + 77,358.5 T^{-1} \quad \begin{matrix} 298.15 < T < 1811 \\ 1811 < T < 6000 \end{matrix}$$

$$= -25,384.451 + 299.31255 T - 46.0 T \ln T + 2.2960305 \cdot 10^{31} T^{-9}$$

$${}^0G_{Cu}^{bcc} - H_{Cu}^{SER} = -3753.46 + 129.23 T - 24.1124 T \ln T - 0.00265684 T^2 + 1.29223 \cdot 10^{-7} T^3 + 52,477.8 T^{-1} \quad \begin{matrix} 298.15 < T < 1358 \\ 1358 < T < 6000 \end{matrix}$$

$$= -9525.3 + 182.549 T - 31.38 T \ln T + 3.64643 \cdot 10^{29} T^{-9}$$

$${}^0L_{Fe,Cu}^{bcc} = 39,676.0 - 4.73222 T$$

$$T_c^{bcc} = 1043 x_{Fe} - 41.4 x_{Fe} x_{Cu}$$

$$\beta^{bcc} = 2.22 x_{Fe}$$

B. Thermodynamic Data

The enthalpy of mixing of the liquid phase has been measured by Oelsen *et al.*^[21] at 1875 K, Podgornik^[29] at 1875 K, Woolley and Elliott^[30] at 1875 K, El'khasan *et al.*^[31] between 1810 and 1910 K, Tozaki *et al.*^[32] for 1833 to 1863 K, and Batalin and Sudavtsova^[33] between 1873 and 1910 K. Results from References 21, 29, 30, and 32, which agree well with one another, are included in the optimization. The data of El'khasan *et al.* are discarded because they exhibit marked temperature dependence, which was later contradicted by both Tozaki *et al.*^[32] and Batalin *et al.*^[33] Measurements by Batalin *et al.*^[33] are not used also, since they exhibit some scatter or unusual compositional dependence.

The partial Gibbs energy data in liquid alloys have been measured by several authors. With vapor pressure measurements, Morris and Zellars^[34] determined the activity of copper in liquid iron at 1825 K, which showed strong positive deviations from Raoult's law. The activities of both Fe and Cu in liquid Fe-Cu alloys at 1873 K were obtained by Maruyama and Ban-ya^[35] using a modified transportation method. Using the electromotive forces (EMF) method, Batalin and Sudavtsova^[33] have determined the partial Gibbs energy of iron in Fe-Cu alloys at 1873 K. Most recently, Timberg *et al.*^[36] determined the activities of Fe and Cu in Fe-Cu alloys by using a high temperature mass spectrometric technique. Although there is a certain amount of scatter in the partial Gibbs energy data obtained from these four sources,

the data are generally in good agreement and were all retained in the selected data set.

The activities of copper in solid iron for several temperatures have been determined by Arita *et al.*^[37] by equilibrating pure iron plates with liquid silver-copper alloys. Since the literature values of the Cu activity in Ag-Cu alloys have to be used in their approach, the results are very likely to be unreliable. Hence, the information was not utilized in our optimization.

IV. RESULTS AND DISCUSSION

The parameters optimized in the present study are summarized in Table I, in which the unary data of Fe and Cu taken from Dinsdale^[6] and the parameters for describing the magnetic contribution to the Gibbs energy of solid phases are also included. With all of these thermodynamic parameters, stable and metastable phase equilibria, T_0 curves, and thermodynamic properties are calculated by using the Thermo-Calc program.^[38] Comparisons with the selected experimental data and previous assessments are elaborated. Predictions of the ranges of possible extension of the solid solubility in this system upon rapid solidification are presented.

A. Thermochemical Properties

The calculated enthalpies of mixing of liquid alloys at 1873 K are compared with the experimental data in Figure 1. A good agreement between the present assessment and the measurements by Oelsen *et al.*,^[21] Podgornik,^[29] Woolley and Elliott,^[30] and Tozaki *et al.*^[32] is obtained. This is in accordance with the evaluated values of Hultgren *et al.*,^[16] which can not be accommodated by Chuang *et al.*^[5] Figure 2 shows the activities of Fe and Cu in liquid solutions. As can be

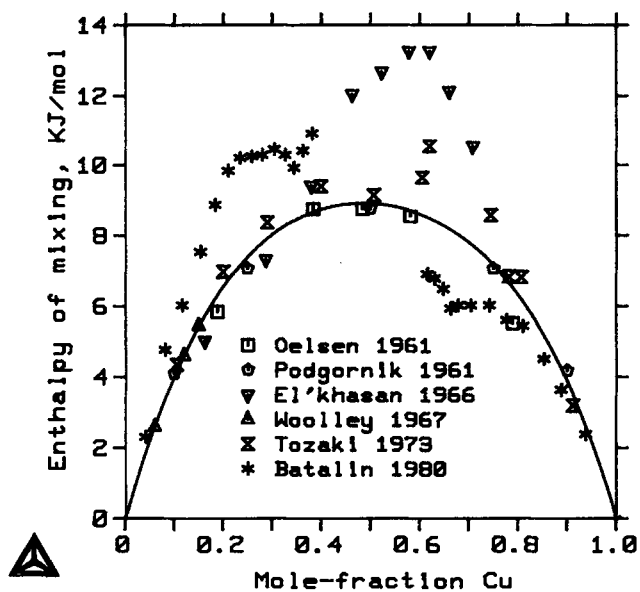


Fig. 1—Comparison between the calculated and experimentally determined enthalpies of mixing of liquid Fe-Cu alloys at 1873 K.

seen, the experimental data from Morris and Zellars^[34] and Maruyama and Ban-ya^[35] are well reproduced.

In their assessment, Chuang *et al.*^[5] has also examined the function α_{Cu} , which is defined as ${}^E\bar{G}_{Cu}^{liq}/(1-x_{Cu})^2$. Through the examination, they found that the calculated values according to Kubaschewski *et al.*^[11] exhibit unusual compositional dependence at low copper concentrations and owe it to the use of a fifth-power term in composition for the excess Gibbs energy description. In the present study, preliminary assessment with the number of parameters for the liquid phase limited to 6 (3 at constant temperature, fourth-power term in composition) was performed, it was found that it was impossible for the high temperature phase diagram data to be accounted for within the experimental uncertainties. So in the final assessment, another parameter leading to x_{Cu}^5 was added. We checked the composition dependence of the α function at 1000, 1250, 1500, 1750, 2000, 2250, 2500, 2750, and 3000 K, no strange behavior was found. It is worth pointing out that this examination makes no assurance of normal behavior for the α function at all temperatures. The unusual behavior might occur in a narrow temperature range. Figure 3 shows that our assessment, without any anomaly, agrees reasonably with the experimental data^[34-36,39,40] at 1873 K within the whole composition range. The calculation of Chuang *et al.*,^[5] with 6 parameters and ensuring normal behavior of the α function at all temperatures yields smaller values. But they are also reasonably well within the uncertainty given by Hultgren *et al.*,^[16] except those at the Fe-rich end.

For the γ phase, the assessed activities of copper are compared with the experimental data in Figure 4. Although the values by Arita *et al.*^[37] were not used in the optimization, they are still well accounted for by the present thermodynamic modelling.

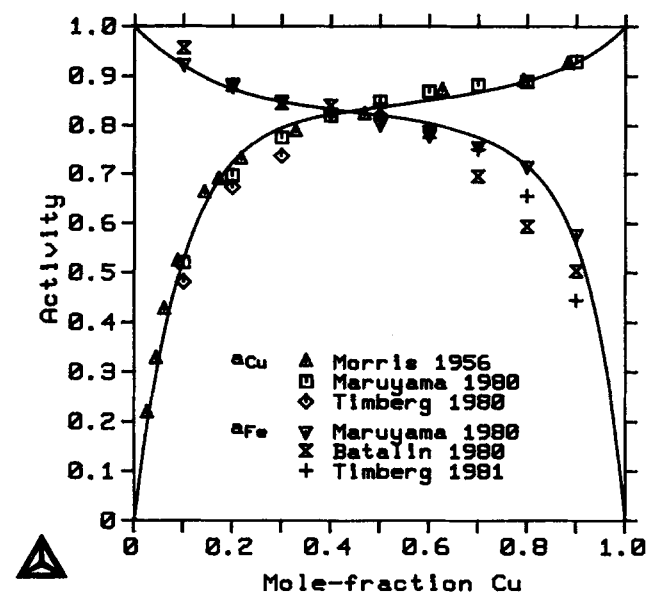


Fig. 2—Comparison between the calculated and experimentally determined activities of Fe and Cu in liquid Fe-Cu alloys at 1873 K.

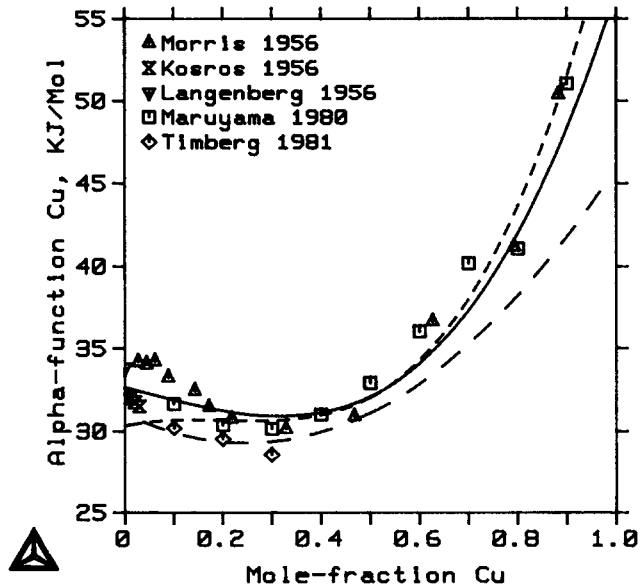


Fig. 3—Comparison between various assessments and measurements for α_{Cu} function in Fe-Cu alloys at 1873 K. The short dashed line is from Kubaschewski *et al.*,^[1] the long dashed line is from Chuang *et al.*,^[5] and the solid line is from the present study.

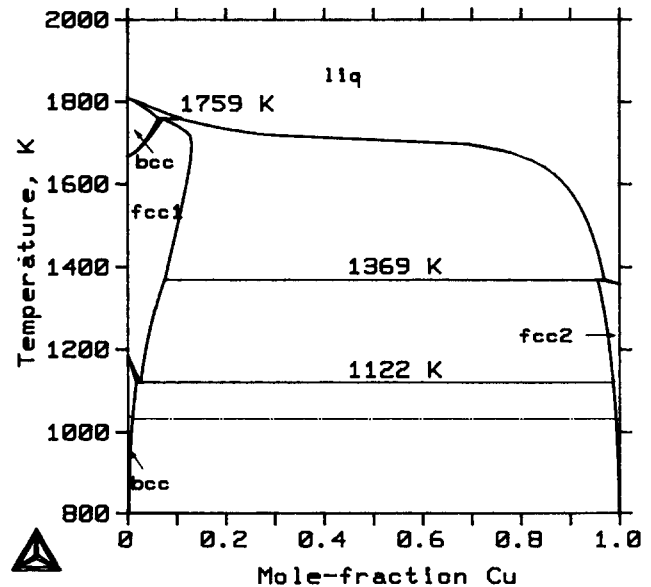


Fig. 5—The Fe-Cu phase diagram calculated from the present thermodynamic description.

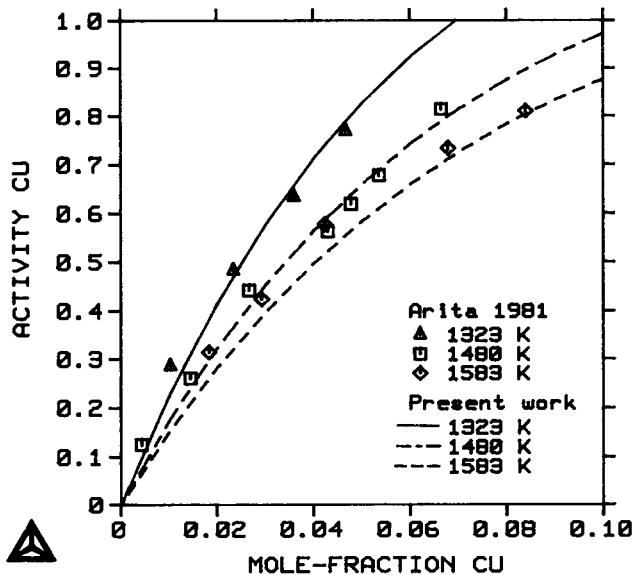


Fig. 4—Comparison between the calculated and experimentally determined activities of Cu in iron-rich γ solutions.

B. The Phase Diagram

The whole Fe-Cu phase diagram according to the present assessment is presented in Figure 5. Comparisons with the available experimental data are given in Table II and Figures 6 through 10.

In Table II, the assessed three-phase equilibria are listed together with the experimental data and previous assessments for comparison, showing that the agreement

between our assessment and the experimental information is satisfactory for the three invariant equilibria and is better than that between the other assessed results and the experimental ones. The peritectic temperatures reported by Hellawell and Hume-Rothery^[19] are both 6 K lower than that measured by Maddocks and Claussen.^[18] Thus, it is reasonable to accept one group's result while assuming a systematic error in temperature to the other. The present study prefers the report of Maddocks and Claussen^[18] because (a) it agrees with Oelsen *et al.*^[21] on the temperature of the peritectic reaction $L + \gamma \rightleftharpoons \epsilon$, and (b) it allows better fit to the liquidus data.

The calculated boundaries for δ /liquid equilibrium are compared with the experimental data in Figure 6. The assessed liquidus for the δ phase agrees with the measured values of Maddocks and Claussen^[18] within the uncertainty of the measurement. The liquidus temperatures determined by Hellawell and Hume-Rothery^[19] are lower than the assessed ones by 6 to 9 K and are closer to the calculated metastable liquidus for the γ phase. Although the possibility cannot be excluded that Hellawell and Hume-Rothery's results are the determination of metastable equilibrium, as assumed by Chuang *et al.*^[5] in their assessment, we think that this possibility is rather remote in view of the experimental conditions in the phase equilibria investigation.^[19] Recalling what was discussed previously about the peritectic temperatures, we believe it is reasonable to explain the discrepancy by suggesting that there is a systematic error of -6 K for temperatures due to unknown reasons in Hellawell and Hume-Rothery's work. Furthermore, if we accept this assumption, the δ solidus data reported by Hellawell and Hume-Rothery will also be well accounted for by the present assessment (Figure 6). The δ solidus data points given by Maddocks and Claussen^[18] are probably too low, even lower than those given by Hellawell and Hume-Rothery.^[19]

Table II. Comparison between the Calculated and Experimental Invariant Equilibria in the Fe-Cu System

$\delta + \text{liq} \rightleftharpoons \gamma$				
T (K)	x_{Cu}^{δ}	x_{Cu}^{γ}	$x_{\text{Cu}}^{\text{liq}}$	Source
1759	—	—	0.098	Maddocks and Claussen ^[18]
1753	—	—	0.098	Hellawell <i>et al.</i> ^[19]
1755	0.061	0.066	0.100	Oelsen <i>et al.</i> ^[21]
1753	0.066	0.080	0.127	Kubaschewski <i>et al.</i> ^[11]
1752	0.063	0.075	0.124	Hasebe and Nishizawa ^[2]
1764	0.064	0.076	0.116	Chuang <i>et al.</i> ^[5]
1759	0.063	0.073	0.108	this work
$\gamma + \text{liq} \rightleftharpoons \varepsilon$				
T (K)	x_{Cu}^{γ}	$x_{\text{Cu}}^{\varepsilon}$	$x_{\text{Cu}}^{\text{liq}}$	Source
1369	—	—	—	Maddocks and Claussen ^[18]
1363	—	—	—	Hellawell <i>et al.</i> ^[19]
1369	0.071	0.955	0.968	Oelsen <i>et al.</i> ^[21]
1369	—	0.952	0.961	Kubaschewski <i>et al.</i> ^[11]
1369	0.090	0.950	0.968	Hasebe and Nishizawa ^[2]
1371	0.076	0.952	0.965	Chuang <i>et al.</i> ^[5]
1369	0.075	0.955	0.968	this work
$\gamma \rightleftharpoons \alpha + \varepsilon$				
T (K)	x_{Cu}^{α}	x_{Cu}^{γ}	$x_{\text{Cu}}^{\varepsilon}$	Source
1124	0.012	0.018	0.985	Oelsen <i>et al.</i> ^[21]
>1115	—	—	—	Wriedt <i>et al.</i> ^[25]
1139	0.019	—	—	Qureshi ^[26]
1124 ± 9	—	0.023	—	Speich <i>et al.</i> ^[23]
1131	0.018	—	—	Salje ^[24]
1124	—	0.018	—	Kubaschewski <i>et al.</i> ^[11]
1126	0.018	0.027	0.986	Hasebe and Nishizawa ^[2]
1118	0.021	0.028	0.987	Chuang <i>et al.</i> ^[5]
1122	0.017	0.026	0.987	this work

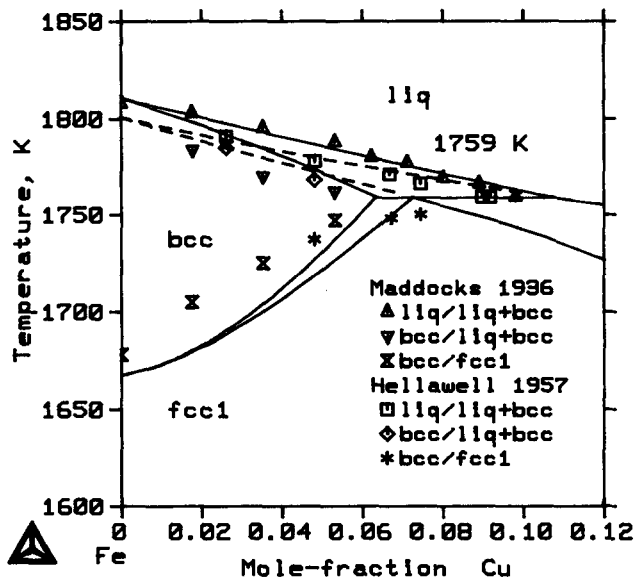


Fig. 6—Comparison between the calculated and experimentally determined phase boundaries in equilibrium with the bcc (δ) phase. The metastable fcc I (γ)/liq equilibrium is shown with the broken lines.

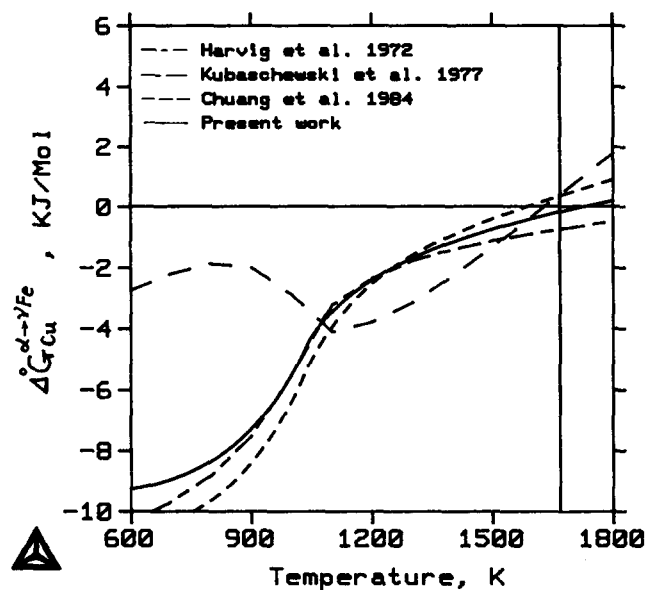


Fig. 7—Assessed results for the effect of copper on the relative stability of the α and γ phases in infinite dilute iron alloys.

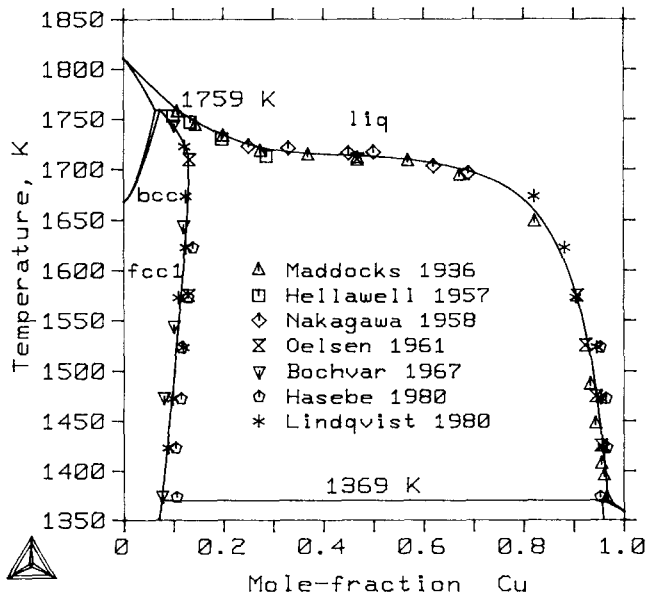


Fig. 8—Comparison between the calculated and experimentally determined fcc 1 (γ) liquidus and solidus.

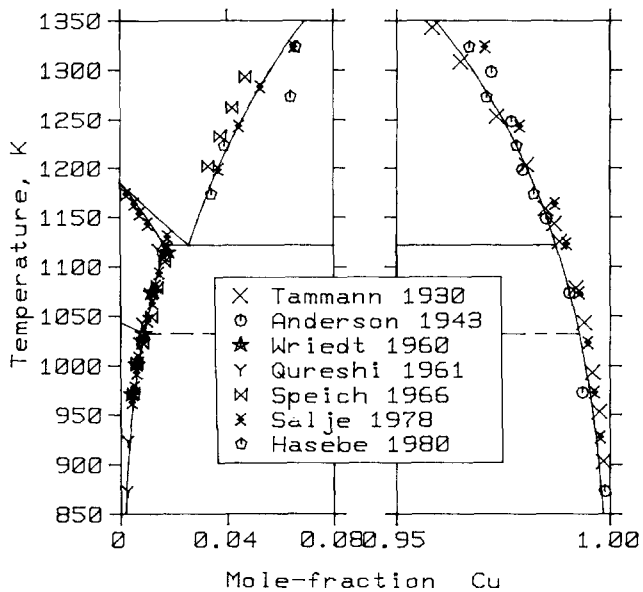


Fig. 9—Comparison between the calculated and experimentally determined phase boundaries below 1369 K.

The δ/γ equilibrium is also shown in Figure 6. The assessed boundary lines with concave curvatures fall well below the experimental points that indicate convex lines. The same kind of disagreement has occurred in the previous assessments^[1,2,5] and is so serious that a minimum point was produced in the two-phase equilibrium. Not long after their first assessment, Hasebe and Nishizawa^[4] reoptimized the interaction parameters for the bcc phase so that the minimum disappears, as they believed that Cu should not stabilize the δ phase but rather the γ phase. The effect of Cu on the relative stability of the δ and γ phases at the infinite dilute iron

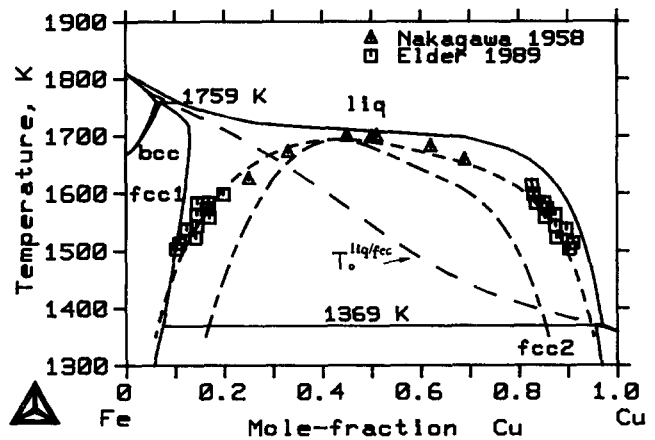


Fig. 10—The calculated metastable liquid binodal and spinodal and liquid/fcc T_0 curve together with experimentally determined boundaries for the metastable liquid miscibility gap.

solutions has been discussed by Harvig *et al.*^[41] and Chuang *et al.*^[5] Here, we only compare the values of the standard free energy of reaction at infinite dilute solutions ($\Delta^0 G_{Cu}^{a \rightarrow \gamma Fe}$)^[41] calculated from the thermodynamic parameters provided in References 1, 5, and 41 and in the present study in Figure 7. According to this assessment, $\Delta^0 G_{Cu}^{a \rightarrow \gamma Fe}$ is negative at 1667 K, so Cu will stabilize the γ phase. In consequence, no minimum appears in our calculated results. Although this is in agreement with the available experimental evidence, the possibility of the existence of a minimum in the δ/γ loop cannot be ruled out fundamentally because we found that it can be realized with a slight modification of the thermodynamic parameters without any noticeable damage to other fits. Further detailed experimental study is necessary to resolve the doubt. Figure 7 also reveals a strange kink in the line calculated with the parameters of Kubaschewski *et al.*,^[1] which is due to their questionable modeling of magnetic contribution. We detected that Eq. [7] in their article is actually different from the formula of Hillert *et al.*,^[42] which they desired to adopt, by an negative sign.

A good agreement between the assessed γ liquidus and the corresponding experimental data is shown in Figure 8. In the composition range $x_{Cu} = 0.3$ to 0.7, the agreement is excellent. Outside this range, all the points measured by cooling curves^[18,19] fall more or less below the assessed liquidus, while those determined by EMPA,^[2,3] except one point, fall on or above the assessed liquidus line. The discrepancies between the results from cooling curves and the calculated values, we think, are due to the supercooling effect, which becomes severe when the solidus and liquidus are farther apart and the liquidus falls more steeply as the percentage of Cu increases.^[43] The γ solidus is also illustrated in Figure 8. The calculated result agrees well with the investigation by Lindqvist and Uhrenius.^[3] Measurements by Hasebe and Nishizawa^[2] and Bochvar *et al.*^[22] gave higher and lower solubilities of copper in γ phase, respectively. Our calculated retrograde point is at $x_{Cu} = 0.13$ and $T = 1698$ K. A good fit of the assessed values

to the experimental data below 1369 K is shown in Figure 9.

The assessed metastable liquid miscibility gap is depicted in Figure 10, from which it can be seen that the experimental data are reasonably accounted for in view of the large uncertainties involved in the experiments.^[20,44] According to the present assessment, the consolute point of the miscibility gap is at $x_{Cu} = 0.43$ and $T_c = 1694$ K.

In Figures 11 and 12, other metastable phase equilibria that might be of practical interest are presented. It is interesting to note that in Figure 11, the metastable liquid/ ϵ equilibrium terminates at a certain temperature, 1382.5 K, where the metastable solidus for ϵ phase reaches the spinodal for the fcc phase. The similar situation goes for the metastable α/γ equilibrium, which is represented in Figure 12. This feature arises from the fact that the single fcc phase is unstable within the spinodal or that the fcc Gibbs energy curve has a negative curvature within the spinodal.^[45]

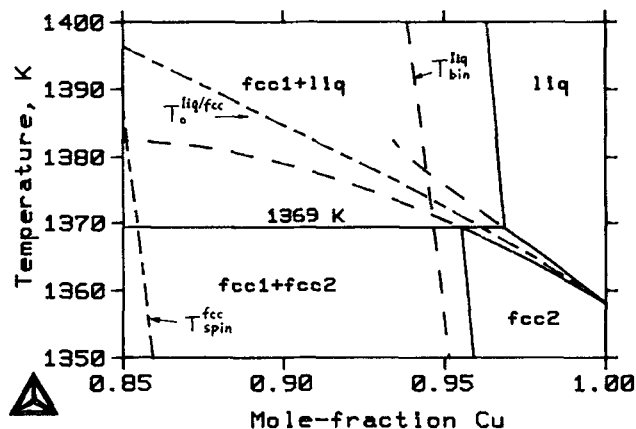


Fig. 11—The calculated metastable liq/fcc 2 (ϵ) equilibrium. The T_0 curve for liq/fcc equilibrium, spinodal for fcc phase and binodal for liquid phase, are also presented.

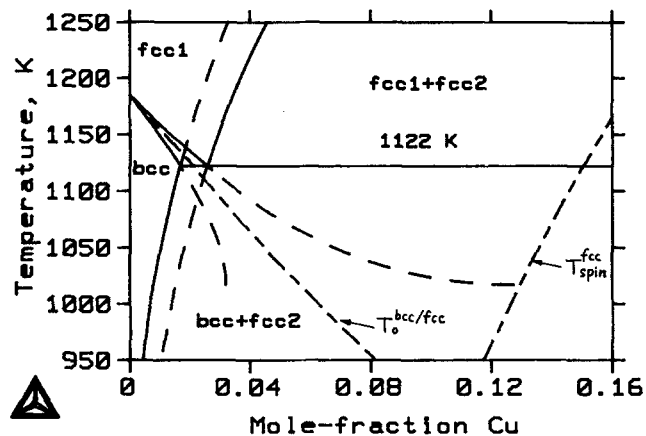


Fig. 12—The calculated metastable bcc (δ)/fcc 1 (γ) equilibrium as well as its T_0 curve. The fcc spinodal is also shown.

C. Limit of Enhanced Solid Solubility upon Rapid Solidification

Although Fe and Cu are almost insoluble in each other at room temperature under equilibrium conditions, largely enhanced solid solubility can be obtained, for instance, by liquid quenching^[48] and vapor quenching.^[49,50] The limit of the extension of solid solubility is determined by thermodynamics and kinetics of phase transformation. Taking advantage of the assessed thermodynamic parameters, we shall try to throw light on this matter from a thermodynamic point of view in this section.

In Figure 10, the calculated T_0 curve for the liquid/fcc equilibrium is superimposed on the metastable liquid binodal and spinodal, together with the stable phase equilibria. This diagram shows that the T_0 curve passes through the spinodal for the liquid phase at $x_{Cu} = 0.325$, $T = 1649$ K and $x_{Cu} = 0.844$, $T = 1398$ K. Within the region bounded by the spinodal, a homogeneous liquid phase is thermodynamically unstable and a solid phase introduced into it cannot grow until after liquid separation.^[45] Therefore, the two intersections, theoretically, shall define the limits of the metastable extension of the solid solubilities of the γ and ϵ phases upon rapid solidification from melt.^[46]

It seems that our prediction has been verified necessarily but not sufficiently by Munitz's experimental observation,^[47] in which he found that the enhanced solute trapping in the γ phase never exceeded about 32.12 at. pct Cu after electron beam surface melting and subsequent self-quenching of Fe-Cu alloys. Nevertheless, the investigator, probably unaware of the two intersections or the implications of them, concluded that what he found indicated a limit to the extent of supercooling that could be obtained under the applied experimental conditions. As a matter of fact, a higher degree of supercooling does not necessarily result in larger extent of enhanced solute trapping in this system.

Another experimental study on the extended solid solubility upon rapid quenching of Fe-Cu liquid alloys has been performed by Klement.^[48] In the absence of any X-ray evidence for Fe-rich α phase, he considered the alloys containing up to 20.0 at. pct Fe as single phase, and consequently he had to think that the maximum in the lattice spacing-composition curve near 7.2 ± 0.5 at. pct Fe is characteristic of the fcc solid solution. However, according to our calculation, it is impossible for the solubility of the ϵ phase to extend beyond 16.6 at. pct Fe by melt quenching. A further analysis of his experimental data on the lattice parameters makes us believe that single phase was obtained by Klement only within the composition range of 0 to 7.2 at. pct Fe. First, as we know, X-ray diffraction analysis does not infallibly identify minor phases, especially those of small amount. Moreover, the band theory of ferromagnetism for Fe alloys predicts that the lattice spacings of the alloys beyond the composition of 8 at. pct Fe should not decrease but may increase more.^[49] Finally, vapor quenching and mechanical alloying results^[49-51] gave no evidence of the maximum of the lattice parameter values. In Figure 13, we extrapolate linearly Klement's data on the dilute alloys (0 to 7.2 at. pct Fe) to the concentration 20 at. pct Fe. It could be seen readily that the

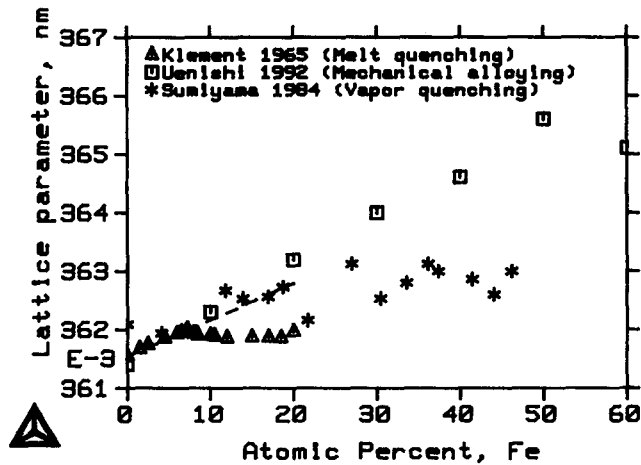


Fig. 13—Lattice parameters of metastable supersaturated Cu-Fe solid solution synthesized by melt quenching,^[48] sputtering,^[49] and mechanical alloying.^[51]

extrapolated value at this composition is in good agreement with the experimental result from Sumiyama *et al.*^[49] So we should say that Klement's experimental values are actually very reliable, but his conclusion may be incorrect. The slightly decreasing lattice spacing of the alloys containing 8 to 20 at. pct. Fe implies that the solid solubility of the ϵ phase becomes a little smaller because of the formation of the Fe-rich α phase in some way.

In a similar study on the Co-Cu system,^[52] the limit of enhanced solid solubility upon melt quenching in the system was also predicted by taking into account the T_0 curve and metastable liquid spinodal. The calculated value is found to be in reasonable agreement with a recently published experimental work.^[53]

Melt quenching of the Fe-Cu alloys can lead to a certain degree of enhanced solute trapping. However, by using vapor quenching methods, such as sputtering or mechanical alloying technique, which bypass the liquid state, the solid solubility can be extended dramatically.^[49-51] In this situation, as Massalski^[54] has pointed out, kinetic considerations determine the ultimate result, but Gibbs energies are of some help. Figure 14 shows the calculated Gibbs energies of the liquid, fcc, and bcc phases in the Fe-Cu system at room temperature together with the experimentally realized ranges of metastable single phases, and it appears that the T_0 principle still holds, by and large, for the prediction of the possible relative ranges of the competing solid phases.

V. SUMMARY

The Fe-Cu system has been critically assessed by using thermodynamic models for the Gibbs energy of various phases. A set of thermodynamic parameters, which allows a general agreement between the calculated and experimental data over the whole composition range above 800 K, has been obtained. Stable and metastable phase equilibria, T_0 curves, and thermochemical properties were calculated. Extension ranges of solid

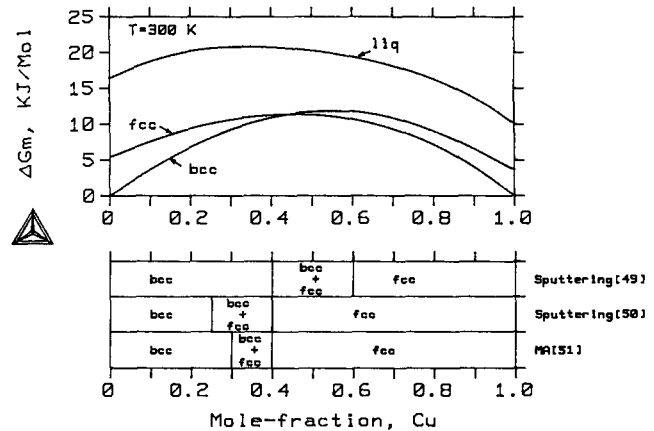


Fig. 14—The calculated Gibbs energy curves at 300 K in the Fe-Cu system according to the present assessment and the experimentally observed ranges of the extended solid solubility.

solubility upon rapid solidification in this system have been discussed.

APPENDIX

An unpublished work by Jansson^[55] can be added to the list of previous assessments. With his parameters, we calculated the phase diagram using Thermo-Calc and compared it with the experimental data. It turned out that the agreement does not seem to be as good as that obtained in the present assessment and in fact even poorer than that reported in an earlier evaluation by Chuang *et al.*^[5] None of the experimentally observed γ solidus data has been reproduced, and the assessed liquidus data above 1710 K deviates from the measured values significantly.

ACKNOWLEDGMENTS

The authors wish to express their gratitude to Dr. Lukas of the Max-Planck Institute for Metals Research, Germany and Dr. Sundman of the Royal Institute of Technology, Sweden for providing the computer software used in this study. Special thanks go to Professor Y.A. Chang of the University of Wisconsin-Madison for constructive discussions. One of the authors (QC) would also like to thank Dr. Yong Du and Mr. Jichen Zhao (now at Tokyo Institute of Technology and Lehigh University, respectively) for valuable help of various kinds.

REFERENCES

1. O. Kubaschewski, J.F. Smith, and D.M. Bailey: *Z. Metallkd.*, 1977, vol. 68, pp. 495-99.
2. M. Hasebe and T. Nishizawa: *CALPHAD*, 1980, vol. 4, pp. 83-100.
3. P.-A. Lindqvist and B. Uhrenius: *CALPHAD*, 1980, vol. 4, pp. 193-200.
4. M. Hasebe and T. Nishizawa: *CALPHAD*, 1981, vol. 5, pp. 105-108.
5. Y. Chuang, R. Schmid, and Y.A. Chang: *Metall. Trans. A*, 1984, vol. 15A, pp. 1921-30.

6. A.T. Dinsdale: *CALPHAD*, 1991, vol. 15, pp. 317-425.
7. L. Kaufman and H. Bernstein: *Computer Calculation of Phase Diagrams*, Academic Press, New York, NY, 1970.
8. G. Inden: *Project Meeting, CALPHAD V*, Max-Planck Institute Eisenforsch, Dusseldorf, Germany, 1976, pp. 1-13.
9. M. Hillert and M. Jarl: *CALPHAD*, 1978, vol. 2, pp. 227-38.
10. A.F. Guillermet and P. Gustafson: *High Temp.-High Pressures*, 1985, vol. 16, pp. 591-610.
11. R. Ruer and F. Goerens: *Ferrum*, 1917, vol. 14, pp. 49-61.
12. H.L. Lukas, E.-Th. Henig, and B. Zimmermann: *CALPHAD*, 1977, vol. 1, pp. 225-36.
13. M. Hansen and K. Anderko: *Constitution of Binary Alloys*, 2nd ed., McGraw-Hill, New York, NY, 1958, pp. 580-82.
14. R.P. Elliott: *Constitution of Binary Alloys*, 1st Suppl., McGraw-Hill, New York, NY, 1965, p. 372.
15. F.A. Shunk: *Constitution of Binary Alloys*, 2nd Suppl., McGraw-Hill, New York, NY, 1969, p. 287.
16. R. Hultgren, P.D. Desai, D.T. Hawkins, M. Gleiser, and K.K. Kelley: *Selected Values of the Thermodynamic Properties of Binary Alloys*, ASM, Metals Park, OH, 1973, pp. 737-41.
17. T.B. Douglas: *J. Res. Natl. Bur. Stand.—A*, 1969, vol. 73A, pp. 451-70.
18. W.R. Maddocks and G.E. Claussen: *Iron Steel Inst. Spec. Rep.* 14, 1936, pp. 97-124.
19. A. Hellawell and W. Hume-Rothery: *Phil. Trans. R. Soc. London*, 1957, vol. A249, pp. 417-59.
20. Y. Nakagawa: *Acta Metall.*, 1958, vol. 6, pp. 704-11.
21. W. Oelsen, E. Schurmann, and C. Florin: *Arch. Eisenhüttenwes.*, 1961, vol. 32, pp. 719-28.
22. A.A. Bochvar, A.S. Ekatoeva, E.V. Panchenko, and Y.F. Sidokhin: *Dokl. Akad. Nauk SSSR*, 1967, vol. 174, pp. 863-64.
23. G.R. Speich, J.A. Gula, and R.M. Fisher: in *The Electron Microprobe*, T. D. Mckinley, K.F.J. Heinrich, and D.B. Witty, eds., John Wiley & Sons, New York, NY, 1966, pp. 525-41.
24. G. Salje and M. Feller-Kniepmeier: *Z. Metallkd.*, 1978, vol. 69, pp. 167-69.
25. H.A. Wriedt and L.S. Darken: *Trans. TMS-AIME*, 1960, vol. 218, pp. 30-36.
26. A.H. Qureshi: *Z. Metallkd.*, 1961, vol. 52, pp. 799-813.
27. G. Tammann and W. Oelsen: *Z. Anorg. Chem.*, 1930, vol. 186, pp. 257-88.
28. A.G.H. Andersen and A.W. Kingsbury: *Trans. AIME*, 1943, vol. 152, pp. 38-47.
29. A. Podgornik, quoted by W. Oelsen, E. Schurmann, and C. Florin: *Arch. Eisenhüttenwes.*, 1961, vol. 32, pp. 719-28.
30. F. Woolley and J.F. Elliott: *Trans. TMS-AIME*, 1967, vol. 239, pp. 1872-83.
31. A. El'khasan, K. Abdel-Aziz, A.A. Vertman, and A.M. Samarin: *Izvest. Akad. Nauk. SSSR, Met.*, 1966, vol. 3, pp. 19-30.
32. Y. Tozaki, Y. Iguchi, S. Ban-ya, and T. Fuwa: in *Chemical Metallurgy of Iron and Steel*, Proc. of the Int. Symp. on Metals Chemistry, Applications in Ferrous Metals, Sheffield, United Kingdom, July 19-21, 1971, Iron and Steel Institute, London, 1973, pp. 130-32.
33. G.I. Batalin and V.S. Sudavtsova: *Izv. Akad. Nauk SSSR, Met.*, 1980, vol. 2, pp. 45-49.
34. J.P. Morris and G.R. Zellars: *Trans. AIME*, 1956, vol. 206, pp. 1086-90.
35. N. Maruyama and S. Ban-ya: *J. Jpn. Inst. Met.*, 1980, vol. 44, pp. 1422-31.
36. L. Timberg, J.M. Toguri, and T. Azakami: *Metall. Trans. B*, 1981, vol. 12B, pp. 275-79.
37. M. Arita, M. Tanaka, K.S. Goto, and M. Someno: *Metall. Trans. A*, 1981, vol. 12A, pp. 497-504.
38. B. Sundman, B. Jansson, and J.-O. Andersson: *CALPHAD*, 1985, vol. 9, pp. 153-90.
39. P.J. Koros and J. Chipman: *Trans. AIME*, 1956, vol. 206, pp. 1402-04.
40. F.C. Langenberg: *Trans. AIME*, 1956, vol. 206, pp. 1024-25.
41. H. Harvig, G. Kirchner, and M. Hillert: *Metall. Trans.*, 1972, vol. 3, pp. 329-32.
42. M. Hillert, T. Wada, and H. Wada: *J. Iron Steel Inst.*, 1967, vol. 205, pp. 539-46.
43. W. Hume-Rothery, J.W. Christian, and W.B. Pearson: *Metallurgical Equilibrium Diagrams*, Institute of Physics, London, 1953, pp. 97-108.
44. S.P. Elder, A. Munitz, and G.J. Abbaschian: *Mater. Sci. Forum*, 1989, vol. 50, pp. 137-50.
45. J.W. Cahn: *Trans. TMS-AIME*, 1968, vol. 242, pp. 166-80.
46. J.H. Perepezko and W.J. Boettinger: *MRS Symp. on Alloy Phase Diagrams*, L.H. Bennett, T.B. Massalski, and B.C. Giessen, eds., Elsevier, Amsterdam, The Netherlands, 1983, vol. 19, pp. 223-40.
47. A. Munitz: *Metall. Trans. B*, 1987, vol. 18B, pp. 565-75.
48. W. Klement, Jr.: *Trans. TMS-AIME*, 1965, vol. 233, pp. 1180-82.
49. K. Sumiyama, T. Yoshitake, and Y. Nakamura: *J. Phys. Soc. Jpn.*, 1984, vol. 53, pp. 3160-65.
50. C.L. Chien, S.H. Liou, D. Kofalt, W. Yu, T. Eagmi, and T.R. McGuire: *Phys. Rev. B*, 1986, vol. 33, pp. 3247-50.
51. K. Uenishi, K.F. Kobayashi, S. Nasu, H. Hatano, K.N. Ishihara, and P.H. Shingu: *Z. Metallkd.*, 1992, vol. 83, pp. 132-35.
52. Q. Chen: Master's Thesis, Central South University of Technology, Changsha, Hunan, People's Republic of China, 1990.
53. X. Zhang and A. Atrens: *Acta Metall. Mater.*, 1993, vol. 41, pp. 563-68.
54. T.B. Massalski: *Metall. Trans. B*, 1989, vol. 20B, pp. 445-73.
55. A. Jansson: SGTE-database, 1987.